Evolution of the mass-transfer processes in nonideal dissipative systems II: Experiments in dusty plasma

O. S. Vaulina, X. G. Adamovich, O. F. Petrov, and V. E. Fortov
Joint Institute for High Temperatures, RAS 125412, Izhorskaya Street, 13/19, Moscow, Russia
(Received 28 December 2007; published 10 June 2008)

The results of the experimental study of mass-transfer processes are presented for dust systems, forming in a laboratory plasma of a radio-frequency capacitive discharge. The validity of the Langevin and Green-Kubo equations for the description of the dynamics of dusty grains in laboratory plasma is verified. A method for simultaneous determination of dusty plasma parameters, such as the kinetic temperature of the grains, their friction coefficient, and characteristic oscillation frequency, is suggested. The coupling parameter of the system under study and the minimal values of the grain charges are estimated. The parameters of the dusty subsystem obtained (diffusion coefficients, pair correlation functions, charges, and friction coefficients of the grains) are compared with the existing theoretical and numerical data.

DOI: 10.1103/PhysRevE.77.066404 PACS number(s): 52.27.Lw, 82.70.Dd

I. INTRODUCTION

A dusty plasma is an ionized gas containing micrometer-size charged grains (macroparticles) of solid matter (dust). This type of plasma is ubiquitous in nature (in space, in molecular dust clouds, in planetary atmospheres) and often appears in a number of technological processes (for example, fuel burning, industrial processing of semiconductors, etc.) [1,2]. Experiments with dusty plasmas are carried out mostly in gas discharges of various types. In a gas-discharge plasma, micrometer-size grains acquire a significant (negative) electric charge, and can form dust structures similar to a liquid or to a solid. Depending on the experimental conditions, these structures can be close to a uniform three-dimensional (3D) or to a nonisotropic quasi-two-dimensional (2D) system, which consist of several (usually from one up to ten) horizontal layers of macroparticles [3–7]. Owing to their size, the dust particles may be video filmed [4–14]. This makes the laboratory dusty plasma a good experimental model, which can be used to study various physical phenomena in systems of interacting particles that attract widespread interest in the physics of nonideal plasmas, as well as in other areas such as plasma chemistry, physics of the atmosphere, medicine, physics of polymers, etc.

A study of the kinetic (transport) coefficients (constants of diffusion, viscosity, thermal conductivity, etc.) for dusty plasmas is of great interest [3–7]. These constants are fundamental parameters that reflect the nature of the interaction potentials and the phase state of the system. When the deviations of the system from statistical equilibrium are small, the kinetic coefficients can be found from Green-Kubo formulas that were established with the help of the theory of Markovian stochastic processes under the assumption of a linear reaction of the statistical system to small perturbations [8,9]. Diffusion is the basic mass-transfer process, which defines the losses of energy (dissipation) in the system. The collisions of grains with the neutral particles of the surrounding gas have a dramatic effect on the dissipation of dust energy in weakly ionized laboratory plasmas.

To correctly simulate the motion of particles in dissipative media (e.g., dusty plasmas), one should use the Langevin molecular dynamics method (LMDM) based on the solution of a system of differential equations with a stochastic force F_{ran} that takes into account the processes leading to the established equilibrium (stationary) temperature T of the macroparticles, which characterizes the kinetic energy of their random (thermal) motion. In this case, a displacement of the jth particle in a uniform medium along one coordinate, $x_j = x_j(t)$, for the time t, under the action of some potential forces F, can be obtained from the Langevin equation (here $F = dU/dx$, where U is the potential energy of a grain; see Ref. [11]).

In a uniform quasiequilibrium medium (when the deviations of the system from its steady state are small), the diffusion constant may be obtained from measurements of the temporal dependencies of the mean-square displacement (MSD) $\langle x_j^2 \rangle$ of the particles,

$$D_{\mathrm{MSD}}(t) = \langle x_j^2 \rangle / (2t), \tag{1a}$$

or from the analysis of velocity autocorrelation functions $\langle V_x(0) V_x(t) \rangle$ (VAFs),

$$D_{\mathrm{GK}}(t) = \int_0^t \langle V_x(0) V_x(t) \rangle, \tag{1b}$$

where $V_x = (dx_j/dt)$. With $t \to \infty$, the second relation (1b) is a particular case of the well-known Green-Kubo (GK) formulas. Here and below, the brackets $\langle\ \rangle$ denote ensemble and time averaging, i.e., the averaging for all time intervals with the duration t. (The latter is necessary to determine the average characteristics of strongly coupled systems correctly [11].) With increasing time, both these mass-transfer functions $D_{\mathrm{MSD}}(t)$ and $D_{\mathrm{GK}}(t)$ tend to the same constant value $D = \lim_{t \to \infty} D(t)$, which corresponds to the conventional definition of the diffusion coefficient.

Analytical solutions of the Langevin equation for two limiting cases (for noninteracting Brownian particles and for the harmonic oscillators) and the results of computer simulations of liquidlike systems by the LMDM have shown that the relations between the mass-transfer functions $D_{\mathrm{MSD}}(t)$ and $D_{\mathrm{GK}}(t)$, the mean-square displacement $\langle x^2 \rangle = \langle x_j^2 \rangle$, and the VAF $\langle V_x(0) V_x(t) \rangle$ may be presented as [11]

$$D_{GK}(t) = \frac{d\{tD_{MSD}(t)\}}{dt} \equiv \frac{1}{2}\frac{d\langle x^2\rangle}{dt}, \tag{2a}$$

$$\langle V_x(0)V_x(t)\rangle = \frac{d^2\{tD_{MSD}(t)\}}{dt^2} \equiv \frac{1}{2}\frac{d^2\langle x^2\rangle}{dt^2}. \tag{2b}$$

The important result of simulations is the fact that the temporal evolutions of the functions $\langle V_x(0)V_x(t)\rangle$, $D_{GK}(t)$, and $D_{MSD}(t)$ functions in liquid systems for short observation times ($t < 2/\omega_c$) are similar to their evolutions for a system of harmonic oscillators, the motion of which may be described by a single characteristic frequency ω_c [11],

$$\langle V_x(0)V_x(t)\rangle = \frac{T}{M}\exp(-\nu_{fr}t/2)[\cosh(\nu_{fr}t\psi) - \sinh(\nu_{fr}t\psi)/\{2\psi\}], \tag{3}$$

$$\frac{D_{GK}(t)}{D_0} = \frac{\exp(-\nu_{fr}t/2)}{\psi}\sinh(\nu_{fr}t\psi), \tag{4}$$

$$\frac{D_{MSD}(t)}{D_0} = \frac{1-\exp(-\nu_{fr}t/2)[\cosh(\nu_{fr}t\psi) + \sinh(\nu_{fr}t\psi)/\{2\psi\}]}{2\xi_c^2\nu_{fr}t}, \tag{5}$$

where M is the mass of a grain, ν_{fr} is the friction coefficient, $D_0 = T/(\nu_{fr}M)$, $\psi = (1-8\xi_c^2)^{1/2}/2$, and $\xi_c = \omega_c/\nu_{fr}$. This frequency ω_c is proportional to the second derivative of a pair interaction potential U_{IP} at the point of the mean interparticle distance l_p [11]:

$$\omega_c = \{|a_0 U''_{IP}(l_p)|/(\pi M)\}^{1/2}. \tag{6}$$

Here $a_0 \equiv 2$ for uniform 3D systems with a body-centered cubic (bcc) lattice in their crystallization phase, and $a_0 \approx 2.7$ for 2D structures forming a hexagonal lattice during their crystallization.

Measurement of the functions $\langle V(0)V(t)\rangle$, $D_{MSD}(t)$, and $D_{GK}(t)$ at short observation times can be used for the diagnostics of dust components in plasma. As all the mentioned functions are connected by Eqs. (2a) and (2b) and uniquely determined by the parameters of the grains (by their temperature T, characteristic frequency ω_c, and friction coefficient ν_{fr}), it is possible to simultaneously determine all these parameters using the best fitting of any one of the measured functions $\langle V(0)V(t)\rangle$, $D_{MSD}(t)$, and $D_{GK}(t)$ by the corresponding analytical function for a harmonic oscillator. The information on T and ω_c allows one to estimate the value of the effective coupling parameter Γ^* and the scaling parameter ξ, which determine the dynamics of grains in the system under study [10–13]:

$$\Gamma^* = a_1 l_p^2 U''_{IP}(l_p)/(2T), \tag{7}$$

$$\xi = |a_2 U''_{IP}(l_p)|^{1/2}(2\pi M)^{-1/2}\nu_{fr}^{-1}, \tag{8}$$

where $a_1 = a_2 \equiv 1$ for 3D systems; $a_1 = 1.5$, $a_2 = 2$ for the 2D case.

Nevertheless, we should note that to apply the results of simulations of particle motions by the LMDM for analysis of dynamics of grains in plasma and to prove the validity of measurements of diffusion constants with the help of the Green-Kubo formula (1b), one needs to examine whether the considered Langevin model is valid under experimental conditions (i.e., to prove the validity of the Markovian approach of the condition of local equilibrium of the dust system and of the assumption of a linear reaction of this system to perturbations). The main objections to the use of the Langevin model in a treatment of the results of real experiments is the possible influence of boundary conditions, external fields, and strong interparticle interactions on the migration of particles and their energy exchange with the surrounding medium (thermostat) [9]. A lot of special questions arise in the interpretation of dusty plasma experiments. These are the influence of the openness of the dusty plasma system and of the irregular distribution of the grains' stochastic energy on the degrees of freedom, including the question as to whether this energy can be used as the main thermodynamic characteristic that describes the kinetic temperature of the dusty component and characterizes the exchange of its energy with a thermostat.

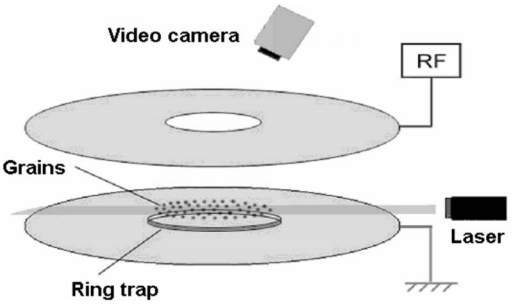

FIG. 1. Simplified scheme of the experimental setup.

Thus, to verify the validity of the Langevin model, we should prove the diffusive character of the grain migration (with $t \to \infty$, $\langle x^2\rangle \propto t$, $D = \text{const}$), and also check the relations (2a) and (2b) that result from simulation of the dynamics of particles using the mentioned Langevin equations. In the case when these relations are valid, the Green-Kubo formula [see Eq. (1b) with $t \to \infty$, $D_{GK}(t) = D_{MSD}(t) \equiv D$] is automatically true.

II. THE DESCRIPTION OF EXPERIMENTS AND THEIR RESULTS

The experiments were carried out for monodisperse grains (with material density $\rho_p \approx 1.5$ g cm^{-3}, radii $a_p \approx 2.75$ and 6.37 μm) in the near-electrode area of a radio-frequency (rf) discharge in argon. The pressure in the discharge was $P = 0.03-0.5$ Torr, and its power $W \approx 2-30$ W. A simplified scheme of the experimental setup is shown in Fig. 1. To visualize the cloud, a flat beam of a He-Ne laser ($\lambda = 633$ nm) was used. The laser illumination had two regimes. In the first, the defocused laser beam illuminated the whole dusty structure inside the trap; this allowed determination of its dimensions. The second regime was used for the detailed observation of the horizontal cross section of the dusty cloud. In this case the laser beam represented a "laser

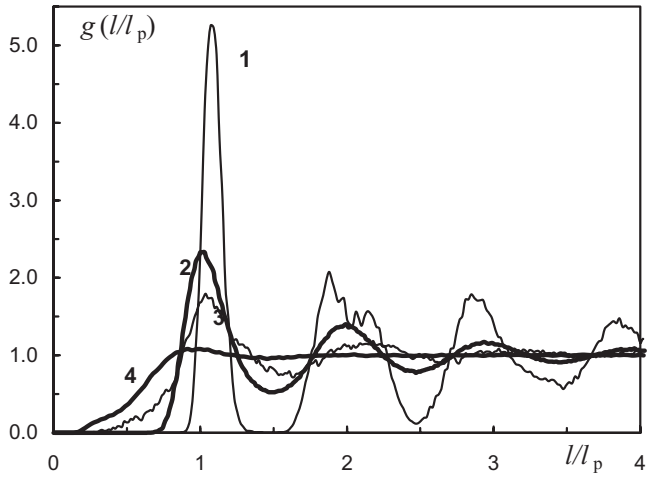

FIG. 2. Pair correlation function $g(l/l_p)$ for various experiments: (1) a_p=6.37 μm, monolayer, P=0.03 Torr; (2) a_p=2.755 μm, monolayer, P=0.35 Torr; (3) a_p=6.37 μm, multilayer system, P =0.11 Torr; (4) a_p=2.755 μm, multilayer system, P=0.04 Torr.

knife" with the width ~2.5 cm and the waist size ~200 μm. The positions of grains were registered with a high-speed complementary metal oxide semiconductor (CMOS) video camera (frame rate f_{VC}=500 s^{-1}). The video recording was processed with special software, which allowed the positions of each particle in the field of view of the video system to be identified. Then the pair correlation functions $g(l)$, the mean intergrain distances, the velocity autocorrelation functions $\langle V(\delta t)V(t)\rangle=[\langle V_x(\delta t)V_x(t)\rangle + \langle V_y(\delta t)V_y(t)\rangle]/2$, the mass-transfer functions $D_{GK}(t)$ and $D_{MSD}(t)$, and the diffusion coefficients D were obtained. The deviations of the measured parameters in the two registered degrees of freedom (x,y) were minor and did not exceed ~0.5–3 %: $\langle V_x(\delta t)V_x(t)\rangle \cong \langle V_y(\delta t)V_y(t)\rangle$, $\langle V_x^2\rangle \cong \langle V_y^2\rangle$, $\langle x^2\rangle \cong \langle y^2\rangle$, where $\delta t = f_{VC}^{-1}$; and the value of the average dust velocities $\langle V_x(t)\rangle \cong \langle V_y(t)\rangle \equiv 0$.

Under the experimental conditions, the dusty structures consisted of several (from one up to ~10) dusty layers, and the observed dusty structures changed from weakly correlated fluids to dust crystals with the mean interparticle distance l_p from ~500 to ~1000 μm. The duration of one experiment under stable conditions was ~5–10 s. The experimental pair correlation functions $g(l)$ for grains of different sizes, forming dusty monolayers and multilayer systems, are presented in Fig. 2. The magnitude of the maximum g_{max} of the functions $g(l)$ and the mean interparticle distance l_p, which was obtained by analysis of the g_{max} position, are given in Table I for different experiments. The random errors of determination of the l_p and g_{max} values were less than 5% for all cases. Nevertheless, we should note that the magnitude of the $g(l)$ peaks may be misrepresented because of (i) the limited number of grains in the field of view of the video camera; and (ii) the probability of simultaneous registration of grains in the next layer in the case of the multilayer structure.

The results of measurement of the velocity autocorrelation functions $\langle V(\delta t)V(t)\rangle$ and mass-transfer functions $D(t)=D_{GK}(t)$ and $D(t)=D_{MSD}(t)$) for various experiments are presented in Figs. 3 and 4, where the normalized values are shown: $f(t)=\langle V(\delta t)V(t)\rangle/V_T^2$ and $D(t)/D_0$, where $V_T^2=T/M$ is the mean square velocity of the stochastic "thermal" motion of grains. The values of V_T^2 and ν_{fr} are presented

TABLE I. Parameters of dusty component for various experiments.

P (Torr)	l_p (mm)	g_{max}	V_T^2 (mm^2/s^2)	D (mm^2/s)	ν_{fr} (s^{-1})	ω_c (s^{-1})	Γ_{3D}/Γ_{2D}	Z_{min}
			a_p=2.75 μm, monolayer					
0.11	1	2.75	0.803	0.0025	30.5	9.7	92/102	5605
0.19	0.84	2.55	0.720	0.002	50.8	9.8	72/80	4303
0.35	0.92	2.35	0.949	0.002	98	8.8	54/60	4478
0.5	0.75	2.7	1.468	0.00135	143	16.3	80/89	6119
			a_p=2.75 μm, multilayer system					
0.04	1.1	1.1	26.3	0.81	11	13.2	6.3/7	8800
0.06	1	1.08	20.1	0.58	15.5	10.23	4.1/4.6	5912
0.1	0.57	1.095	20.7	0.3	34	22.44	6.2/6.9	5581
0.14	0.6	1.05	43.1	0.66	44	15.62	1.6/1.8	4195
			a_p=6.37 μm, monolayer					
0.03	1	5.25	0.45	$\rightarrow 0$	3.5	13.0	293/326	26311
0.05	1	2.45	1.78	0.022	6	12.5	69/77	25396
0.08	0.88	2.75	1.23	0.01	8.4	13.5	90/100	22642
0.42	0.57	4.9	0.73	$\rightarrow 0$	44	27.3	262/291	23852
			a_p=6.37 μm, multilayer system					
0.05	0.92	1.28	12.94	0.449	7	14	10/11	24964
0.07	0.82	1.74	4.51	0.095	8.2	16.4	31.5/35	24742
0.08	0.85	2	2.90	0.048	8.25	15	44/49	23883
0.11	0.88	1.66	4.97	0.12	11.8	13.1	21/23	21968

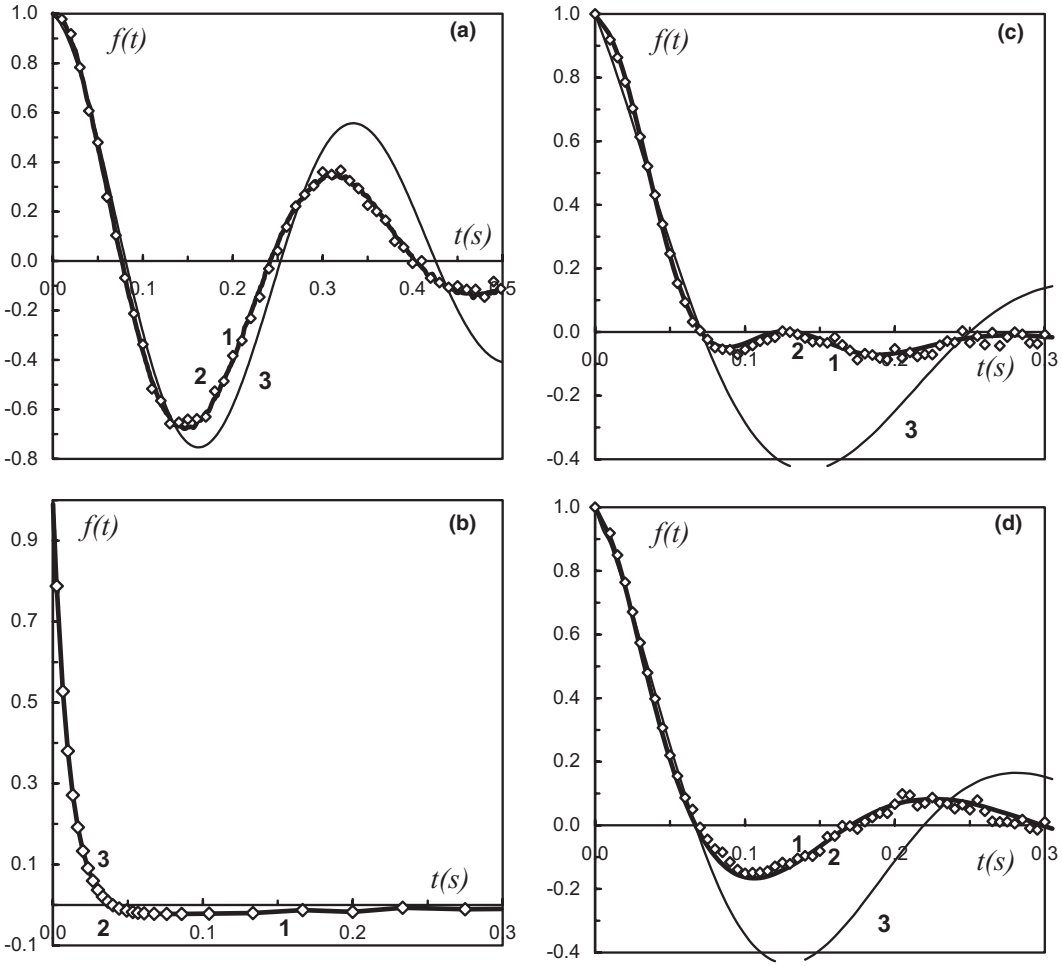

FIG. 3. Velocity autocorrelation function $f(t)$ (curve 1, line), and its value obtained from Eq. (2b) (curve 2, ◇), for various experiments: (a) a_p=6.37 μm, monolayer, P=0.03 Torr; (b) a_p=2.755 μm, monolayer, P=0.35 Torr; (c) a_p=6.37 μm, multilayer system, P =0.11 Torr; (d) a_p=2.755 μm, multilayer system, P=0.04 Torr.Curve 3 is the $f(t)$ function for the harmonic oscillator, Eq. (3), with parameters indicated in Table I.

in Table I, and the methods of their determination are discussed in the next section.

For most experiments, the motion of grains was diffusive: with increasing time $(t\to\infty)$, the mass-transfer functions tended to the same value, $D_{\mathrm{GK}}(t)\approx D_{\mathrm{MSD}}(t)\to D$, excluding the crystalline dusty structures, where with $t\to\infty$, the value of the mean square displacement of a grain from its equilibrium position $\langle x^2\rangle\cong\langle y^2\rangle\to$const and D=const$\to$0. The measured value of the diffusion coefficient D is given in Table I. The difference between the diffusion constants determined from the Green-Kubo formula (1b), $D=D_{\mathrm{GK}}(t\to\infty)$, and from the analysis of the mean square displacements, $D=D_{\mathrm{MSD}}(t\to\infty)$ (1a), did not exceed 5%, which corresponds to the random error. The systematic errors in determination of D due to the finite duration of the measurements were the same ($\leq$5%). The time t_D of establishing the constant value of D ($\pm$5%) was from $\sim$1 to 5 s depending on the gas pressure P (with increase of P, the t_D value also increases). At low pressure P ($\xi_c^3\geq 1$), the $D_{\mathrm{MSD}}(t)$ function achieves its constant value D faster than the $D_{\mathrm{GK}}(t)$ function [see Figs. 4(a), 4(c), and 4(d)]; otherwise with the higher pressure P [$\xi_c\ll 1$, the case of nonoscillating $D_{\mathrm{GK}}(t)$], the $D_{\mathrm{GK}}(t)$ value tends to the constant value faster than $D_{\mathrm{MSD}}(t)$, which allows one to measure the diffusion coefficient D from the Green-Kubo formula in a shorter time [see Fig. 4(b)].

We emphasize that under the conditions of our experiments we have not observed the anomalous or superdiffusion that has been investigated in a set of works [4,15]. With increase of time t $(t\to\infty)$, both mass-transfer functions tended to the same value, $D_{\mathrm{GK}}(t)\approx D_{\mathrm{MSD}}(t)\to D$; i.e., the mean square displacements of particles were proportional to the time t for all presented experiments [see curves 1 and 2 in Figs. 4(a)–4(d)].

The results of examination of the relation between the VAFs $\langle V(\delta t)V(t)\rangle$, mass-transfer functions $D_{\mathrm{GK}}(t)$ and $D_{\mathrm{MSD}}(t)$, and the mean-square displacement $\langle\Delta l^2\rangle=\langle x^2\rangle+\langle y^2\rangle$ are presented in Figs. 3 and 4. In all cases good agreement was obtained between the direct measurements of the functions $\langle V(\delta t)V(t)\rangle$ and $D_{\mathrm{GK}}(t)$ and those functions calculated from the measurements of $\langle\Delta l^2\rangle$ using Eqs. (2a) and (2b). Thus, we can reason that the stochastic model given by the system of Langevin equations allows a correct description of the dust motion under experimental conditions.

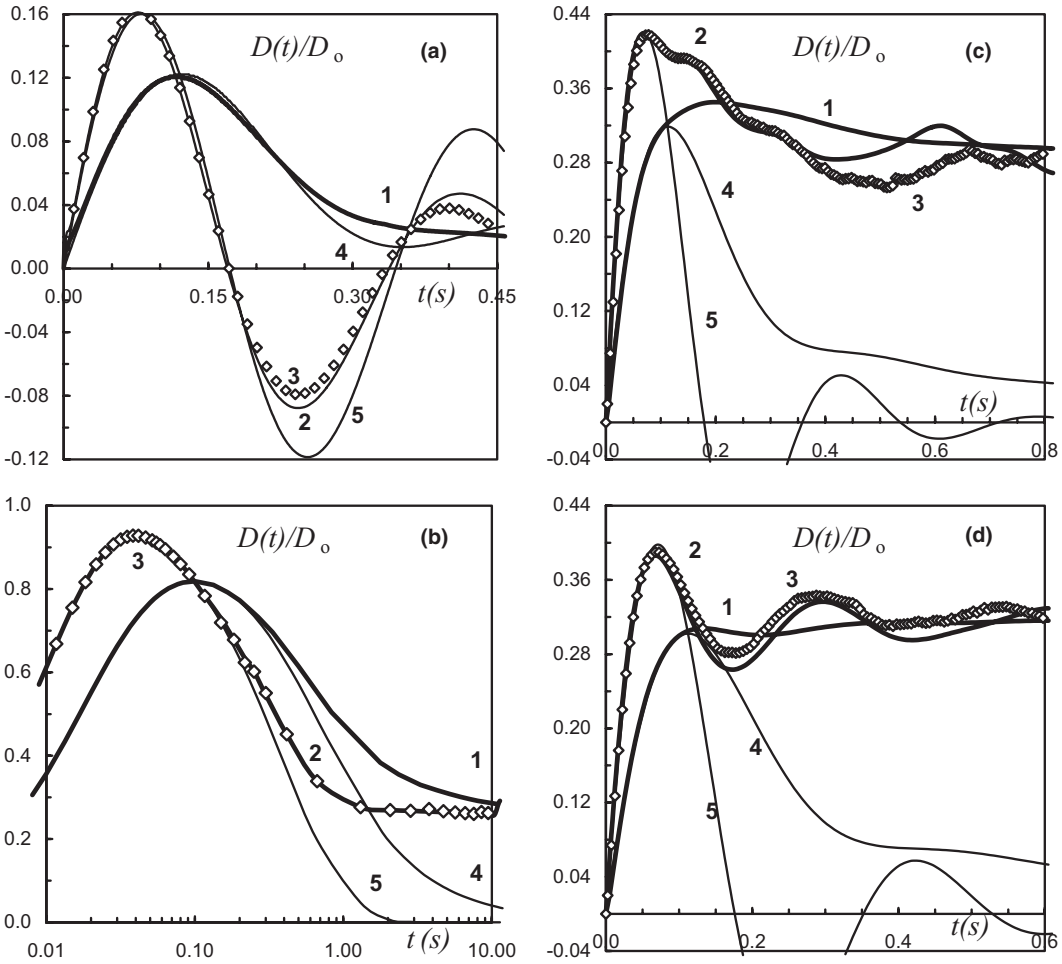

FIG. 4. Mass-transfer evolution functions $D(t)/D_0$: (curve 1, line) $D(t) \equiv D_{\mathrm{MSD}}(t)$; (curve 2, line) $D(t) \equiv D_{\mathrm{GK}}(t)$, Eq. (1b); (curve 3, $\diamond$) $D(t) \equiv D_{\mathrm{GK}}(t)$, Eq. (2a), for various experiments. (a) a_p=6.37 μm, monolayer, P=0.03 Torr; (b) a_p=2.755 μm, monolayer, P=0.35 Torr; (c) a_p=6.37 μm, multilayer system, P=0.11 Torr; (d) a_p=2.755 μm, multilayer system, P=0.04 Torr. Curve 4, Eq. (5), and curve 5, Eq. (4), are the corresponding functions for the harmonic oscillator with parameters indicated in Table I.

III. THE DETERMINATION OF PARAMETERS OF THE DUSTY SUBSYSTEM

The parameters of the macroparticles (the mean square velocity V_T^2 of their stochastic "thermal" motion, the characteristic frequency ω_c, and the friction coefficient ν_{fr}) are presented in Table I. These parameters were obtained by the best fitting of the measured functions $\langle V(\delta t)V(t)\rangle$, $D_{\mathrm{MSD}}(t)$, and $D_{\mathrm{GK}}(t)$, and the corresponding analytical solutions, Eqs. (3)–(5), for the harmonic oscillator. The results of this procedure for various experiments are shown in Figs. 3 and 4. Note that the measured functions presented in these figures are relative, namely, they are the normalized values $f(t) = \langle V(\delta t)V(t)\rangle / V_T^2$ (see Fig. 3), and $D(t)/D_0$ (Fig. 4). The errors in determination of these relative functions for the same intervals of time $t=(t'-t_0)$ were less than 2–3 % for various initial times t_0 which were chosen for processing the experimental results. These random errors may be related to the fluctuations of dusty plasma parameters during experiments they were less than the errors in the determination of the dusty plasma parameters $(V_T^2, \nu_{\mathrm{fr}}, \omega_c)$ by the best fitting of experimental data to the analytical solutions as discussed below.

The errors of the determined parameters were ~5–7 % for V_T^2, less than 10% for the friction coefficient ν_{fr}, and less than 5% for ω_c. To optimize the procedure of fitting the experimental data, the initial values of ω_c and ν_{fr} were chosen in accordance with analytical approximations for the dependence of the maximum $D_{\max}$ of the function $D_{\mathrm{MSD}}(t)$ and the position of this maximum $t_{\max}$ on the parameter $\xi_c = \omega_c / \nu_{\mathrm{fr}}$, which were proposed in [13,14]:

$$D_{\max} \approx D_0/(1+2\xi_c), \tag{9}$$

$$t_{\max}\nu_{\mathrm{fr}} \approx 4\sqrt{2}\pi/(1+8\sqrt{2}\xi_c). \tag{10}$$

The accuracy of these approximations is about 5%. Equation (10) can also be used for choosing the frame rate f_{VC} of the video camera (registering the positions of the grains) and the duration of measurement t_D which are necessary for the correct determination of the dust parameters and diffusion coefficients D. So, the f_{VC} value should be much higher than $1/t_{\max}$, and the duration t_D of measurement for determination of D should satisfy the condition $t_D \gg t_{\max}$. The preliminary estimation of values of ω_c and ν_{fr} under the experimental

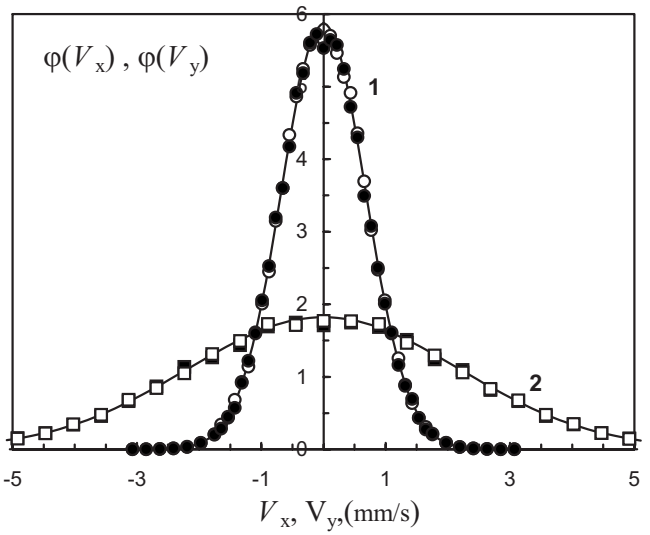

FIG. 5. Measured distribution of the velocities $\varphi(V_x)$ (●;■) and $\varphi(V_y)$ (○;□) for particles of radius a_p=6.37 μm and various experiments: (●;○) monolayer, P=0.03 Torr; (■;□) multilayer system, P=0.11 Torr. Best-fit Maxwellian distributions are also shown with $V_T^2 = T/M$ equal to (1) 0.46 and (2) 4.8 mm^2/s^2.

conditions may be performed using existing theoretical models.

For all cases, the retrieved values of the mean square velocity $V_T^2 = T/M$ were in accordance with the fitting of the velocity distributions $[\varphi(V_x),\ \varphi(V_y)]$ by Maxwellian functions (see Fig. 5). The difference between the values of V_T^2 obtained by the two different methods did not exceed 5–7 % and, in most cases, was within the limits of experimental error.

The retrieved values of ν_{fr} were in good agreement with their theoretical estimations using the free-molecule approximation that under experimental conditions (for argon at room temperature) may be presented as ν_{fr} (s^{-1}) $\approx$[1144P (Torr)]/[a_p (μm)$\times\rho_p$ (g/cm^3)] [16,17]. The difference between the measured and theoretical values of ν_{fr} was less than 12% for all experiments.

For direct examination of the accuracy of the retrieved values for characteristic frequencies ω_c, we need information on the form of the pair potential U_{IP} [see Eq. (6)]. Nevertheless, as the data on the dust parameters (ω_c, V_T^2, and l_p in Table I) allow one to estimate the value of the effective coupling Γ^* and scaling ξ parameters [see Eqs. (6)–(8)], we can compare the measured magnitudes of the maxima g_{max} for the pair correlation functions and of the diffusion coefficients D with existing numerical data. The values of Γ^*, obtained from solving Eqs. (6) and (7), are presented in Table I. For the case of a monolayer the value of $\Gamma^*=\Gamma_{2D}$ was determined in the 2D approach (a_0=2.7, a_1=1.5, a_2=2). For multilayer systems the estimations were performed for two limiting cases: for the 3D case $\Gamma^*=\Gamma_{3D}$ (a_0=2, $a_1=a_2\equiv 1$), and for the 2D case $\Gamma^*=\Gamma_{2D}$ (a_0=2.7, a_1=1.5, a_2=2).

A comparison of the experimental values of the maxima g_{max} and of the normalized diffusion coefficient $D^*=\nu_{fr}D(1+\xi)M/T$ with the results obtained via the numerical simulation for the 3D problem [11] and the monolayer [12,13], is

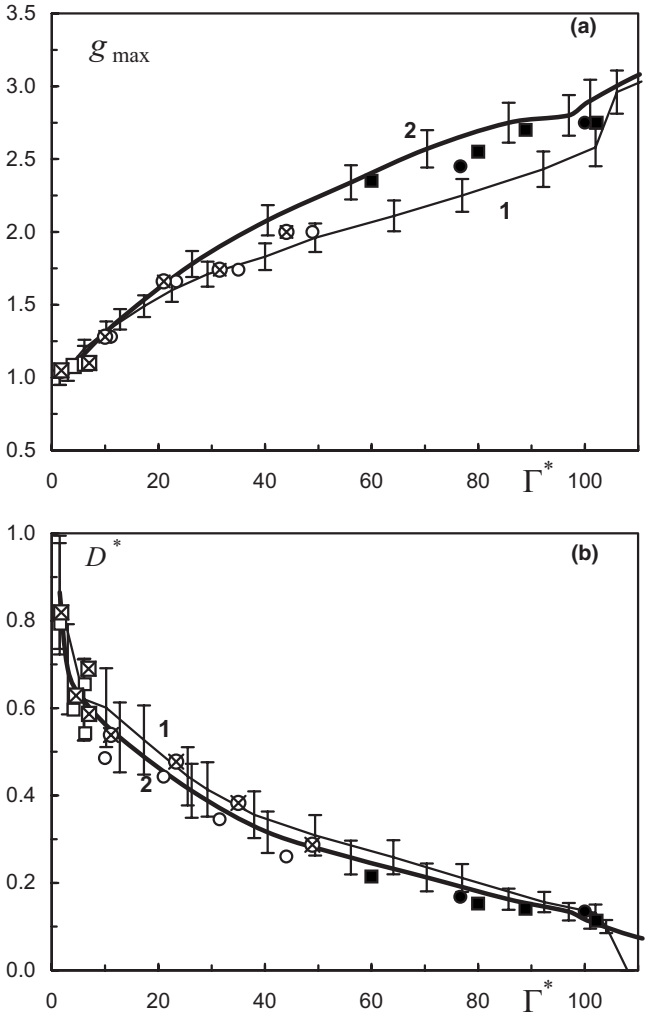

FIG. 6. Maximum g_{max} (a) of the $g(l)$ function and the normalized diffusion coefficient $D^*=D(\nu_{fr}+\omega^*)M/T$ (b) vs Γ^* for (1) 3D systems [11]; (2) monolayers [12,13]. The symbols are the experimental results for grains of radius a_p (○;●;⊗) 6.37 μm, (□;■;⊠) 2.755 μm, that form a dusty monolayer (●;■) or multilayer structure (○;□;⊗;⊠). For the multilayer structure the values of ω^* and Γ^* were determined for two cases: (○;□) 3D system, $\Gamma^*=\Gamma_{3D}$; (⊗;⊠) 2D system, $\Gamma^*=\Gamma_{2D}$.

shown in Figs. 6(a) and 6(b). (Here we note that the 2D and 3D systems were simulated in [11,12] for a wide range of pair isotropic potentials, and in [13] for quasi-2D Yakawa systems.) It is easy to see that the measured dependence $g_{max}(\Gamma^*)$ is in good agreement with the numerical data [see Fig. 6(a)]. The difference between them is at the limits of the experimental (~5%; see Sec. II) and numerical (~5% [11–13]) errors in the determination of g_{max}. The values of the errors are shown in Fig. 6(a) as a 5% confidence interval. The measured dependence $D^*(\Gamma^*)$ is also in good agreement with the numerical data for all considered experiments [Fig. 6(b)]. The deviations between the experimental and numerical values of D^* do not exceed the experimental (~10%; see Sec. II), and numerical error, δ_{cal}, in the determination of D; the δ_{cal} value increases from 7% to 15% when Γ^* varies from ~100 to ~5 [11–13].

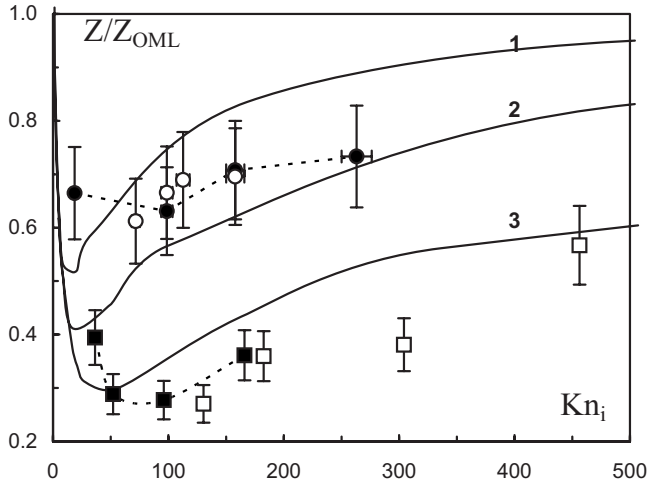

FIG. 7. Calculated dependence of Z/Z_{OML} (lines) on Kn_i for various a_p/λ: (1) 0.07, (2) 0.023, and (3) 0.007. Symbols are the $Z_{\min}/Z_{\mathrm{OML}}$ values for grains of radius a_p (○;●) 6.37 μm and (□;■) 2.755 μm that form a dusty monolayer (●;■) or a multilayer structure (○;□).

The value of the minimum charge $Z=Z_{\min}$ that a grain can acquire in plasma may be obtained under the assumption that the surrounding plasma does not screen the interaction between grains. Thus, in the case of a Coulombic interparticle interaction, we obtain $Z_{\min}\cong\omega_c(\pi M l_p^3/5.4)^{1/2}$ [see Eq. (6)]. The values of $Z_{\min}$ are presented in Table I. The error of this estimation of $Z_{\min}$ is determined by the experimental errors of ω_c and l_p and is about 13%.

The ratio of $Z_{\min}$ to the grain charge $Z_{\mathrm{OML}}\approx(2.7a_pT_e/e^2)$ obtained in the orbital-motion-limited (OML) approach is shown in Fig. 7 versus the Knudsen number $\mathrm{Kn}_i=l_{\mathrm{in}}/a_p$ (in means ion-neutral). Here $T_e=3$ eV is the electron temperature typical for rf discharge in argon [17,18], $l_{\mathrm{in}}=[8T_i/(\pi m_i\nu_{\mathrm{in}}^2)]^{1/2}$ is the ion mean free path between collisions with the gas neutrals, ν_{in} $(\mathrm{s}^{-1})\cong 8\times 10^6 P$ (Torr) is the effective frequency of these collisions for single-charged argon ions [17,18], $T_i\cong 0.026$ eV is their temperature, and m_i is the mass. The results of numerical simulations [19] of the charging of a single spherical particle in a weakly ionized argon-discharge plasma when the drift ion velocity V_{ID} is neglected are also presented in Fig. 7 as the ratio Z/Z_{OML} for various values of $a_p/l=0.07$, 0.023, and 0.007; here $\lambda\approx\lambda_{\mathrm{Di}}=[T_i/(4\pi e^2 n_i)]^{1/2}$ (Di means Debye-ion and marks the ion Debye radius), and n_i is the concentration of ions ($\sim 10^7-5\times 10^8$ cm^{-3}). A simple quantitative comparison of the presented numerical results $Z(\mathrm{Kn}_i)$ with the experimental data $Z_{\min}(\mathrm{Kn}_i)$ is incorrect for at least two reasons. The first is the neglect of the dust screening, whose presence can make the observed $Z_{\min}$ much lower than the real grain charge. The second reason is the neglect of the ion drift velocity V_{ID} in the numerical simulations [19], which may be not be appropriate for the conditions of the considered experiments in the near-electrode area of a rf discharge. In spite of that, we should note the good qualitative agreement between the numerical $Z(\mathrm{Kn}_i)$ and experimental $Z_{\min}(\mathrm{Kn}_i)$ dependencies.

IV. CONCLUSION

The results of an experimental study of mass-transfer processes are presented for dust systems formed in a laboratory plasma of a radio-frequency capacitive discharge. The experiments were carried out for macroparticles of various sizes ($a_p\approx 2.75$ and 6.37 μm) within a wide range of coupling parameters of the dusty subsystem. The velocity autocorrelation functions, mass-transfer functions, diffusion coefficients, pair correlation functions, and concentration were measured. For most experiments, the motion of grains has a diffusive character. The diffusion coefficients D were determined from the Green-Kubo relation and from the mean square displacement of particles. The difference between the values of D obtained by the two different methods did not exceed 5% and was within the limits of experimental error.

In all the cases a good agreement was obtained between the direct measurements of the velocity autocorrelation and mass-transfer functions and those functions calculated from the mean square displacement of particles using Eqs. (2a) and (2b). This means that the stochastic model, given by the system of Langevin equations, can be used for the correct description of the motion of dust under experimental conditions.

The method of simultaneous determination of dusty plasma parameters, such as the kinetic temperature of grains, their friction coefficient, and the characteristic oscillation frequency is proposed. The parameters of the dust were obtained by the best fitting of the measured velocity autocorrelation and mass-transfer functions, and the corresponding analytical solutions for the harmonic oscillator. The coupling parameters of the systems under study and the minimal values of the grain charges are estimated. The parameters of the dusty subsystem obtained (diffusion coefficients, pair correlation functions, charges, and friction coefficients of the grains) are compared with the existing theoretical and numerical data.

ACKNOWLEDGMENTS

This work was partially supported by the Russian Foundation for Fundamental Research (Project No. 07-08-00290), by the Program of the Presidium of RAS, and by the Russian Science Support Foundation.

[1] M. H. Thoma *et al.*, Am. J. Phys. **73**, 420 (2005).
[2] G. E. Morfill, V. N. Tsytovich, and H. Thomas, Plasma Phys. Rep. **29**, 1 (2003).
[3] S. Nunomura, D. Samsonov, S. Zhdanov, and G. Morfill, Phys. Rev. Lett. **96**, 015003 (2006).
[4] S. Ratynskaia, K. Rypdal, C. Knapek, S. Khrapak, A. V. Milanov, A. Ivlev, J. J. Rasmussen, and G. E. Morfill, Phys. Rev. Lett. **96**, 105010 (2006).
[5] V. Nosenko and J. Goree, Phys. Rev. Lett. **93**, 155004 (2004).
[6] A. Gavrikov *et al.*, Phys. Lett. A **336**, 378 (2005).
[7] S. Nunomura, D. Samsonov, S. Zhdanov, and G. Morfill, Phys. Rev. Lett. **95**, 025003 (2005).
[8] N. H. March and M. P. Tosi, *Introduction to Liquid State Physics* (World Scientific, Singapore, 1995).
[9] A. A. Ovchinnikov, S. F. Timashev, and A. A. Belyy, *Kinetics of Diffusion Controlled Chemical Processes* (Nova Science, Commack, NY, 1989).
[10] O. S. Vaulina and S. V. Vladimirov, Phys. Plasmas **9**, 835 (2002).
[11] O. S. Vaulina and X. G. Adamovich (unpublished).
[12] O. S. Vaulina, S. V. Vladimirov, O. F. Petrov, and V. E. Fortov, Phys. Plasmas **11**, 3234 (2004).
[13] O. S. Vaulina and I. E. Drangevski, Phys. Scr., T **73**, 577 (2006).
[14] O. S. Vaulina, O. F. Petrov, and V. E. Fortov, JETP **99**, 711 (2005).
[15] Wen-Tau Juan and Lin I, Phys. Rev. Lett. **80**, 3073 (1998); Bin Liu and J. Goree, *ibid.* **100**, 055003 (2008).
[16] E. M. Lifshitz and L. P. Pitaevskii, *Physical Kinetics* (Pergamon, Oxford, 1981).
[17] Yu. P. Raizer, *Gas Discharge Physics* (Springer, Berlin, 1991).
[18] Yu. P. Raizer, M. N. Shneider, and N. A. Yatsenko, *Radio-Frequency Capacitive Discharges* (CRC, Boca Raton, FL, 1995).
[19] O. S. Vaulina, A. Yu. Repin, O. F. Petrov, and K. G. Adamovich, JETP **102**, 986 (2006).